GEOPHYSICAL RESEARCH LETTERS, VOL. 21, NO. 20, PAGES 2191-2194, OCTOBER 1, 1994

Effect of recent revisions to the geomagnetic reversal time scale on estimates of current plate motions

Charles DeMets[1], Richard G. Gordon[2], Donald F. Argus[3], and Seth Stein[2]

Abstract. Recent revisions to the geomagnetic time scale indicate that global plate motion model NUVEL-1 should be modified for comparison with other rates of motion including those estimated from space geodetic measurements. The optimal recalibration, which is a compromise among slightly different calibrations appropriate for slow, medium, and fast rates of seafloor spreading, is to multiply NUVEL-1 angular velocities by a constant, α, of 0.9562. We refer to this simply recalibrated plate motion model as NUVEL-1A, and give correspondingly revised tables of angular velocities and uncertainties. Published work indicates that space geodetic rates are slower on average than those calculated from NUVEL-1 by 6±1%. This average discrepancy is reduced to less than 2% when space geodetic rates are instead compared with NUVEL-1A.

Introduction

Global models of plate motions averaged over the past few million years (Myr) are a useful standard for comparison with motions averaged over much shorter intervals, especially motions estimated from space geodetic measurements over approximately the past decade. In the past few years, the most widely used standard has been global plate motion model NUVEL-1 [*DeMets et al.*, 1990]. Recent revisions to the geomagnetic reversal time scale [*Shackleton et al.*, 1990; *Hilgen*, 1991ab], which are in better agreement with the observed spacing of marine magnetic anomalies across spreading centers (*Wilson* [1993a]; see also *Gordon* [1993]), suggest that the ages for geomagnetic reversals used in calibrating NUVEL-1 [i.e., those of *Harland et al.*, 1982, which are the same as those of *Mankinen and Dalrymple*, 1979] are systematically too young. Therefore, angular speeds in NUVEL-1 are systematically too fast. Herein we present and discuss a recalibration of NUVEL-1 to remedy this systematic error by multiplying all NUVEL-1 angular velocities by a recalibration factor, α, of 0.9562. Tables describing this recalibrated model, which we refer to as NUVEL-1A, are also presented.

The Effect of Time Scale Adjustments on Estimates of Spreading Rates

Aware that the time scale might eventually require adjustment, *DeMets et al.* [1990] previously sought to estimate spreading rates over as uniform a time interval as possible. If the time interval had been completely uniform and if the beginning of the time interval coincided with a magnetic reversal, revised spreading rates could now be found simply by multiplying the old rates by the ratio of the former to the current estimated age of that reversal. Herein we refer to this recalibration ratio as α.

The needed revision is not this simple, however. Magnetic anomalies corresponding to narrow polarity chrons can be resolved across fast-spreading centers, but not across slow-spreading centers. *DeMets et al.* [1990] estimated spreading rates by adjusting synthetic magnetic-anomaly profiles to fit the narrowest feature that could be resolved in the middle of the anomaly 2A sequence, which corresponds to the Gauss Normal Polarity Chron (Figure 1). Therefore the age corresponding to the magnetic-anomaly feature that was fitted depended upon the broad classification of the rate as slow, medium, or fast. For slow spreading rates ($\lesssim$ 25 mm/yr), all of anomaly 2A was fitted because neither of the sub-chrons within chron 2A (i.e., the Kaena and Mammoth events) can be resolved in the anomaly (Figure 2). For medium spreading rates (between ~25 and ~55 mm/yr), the two reversed subchrons within chron 2A are manifested as a single, small negative anomaly within anomaly 2A, which is the feature that was fitted. For fast spreading rates ($\gtrsim$ 55 mm/yr), the two reversed subchrons within chron 2A are manifested as distinct small negative anomalies; the small positive anomaly between them was fitted.

Because the estimates of the ages of the reversals bounding each of these chrons or sub-chrons have been revised by different fractional amounts (Figure 1), the fractional revisions for slow, medium, and fast spreading differ slightly. Slow rates used in NUVEL-1 should be multiplied by a value for α of 0.9515, medium rates by 0.9529, and fast spreading rates by 0.9573. The uncertainties in these corrections are poorly known and these corrections may differ insignificantly. If, for example, the 95% uncertainty of a reversal age is 20,000 years, then these ratios differ insignificantly. If, on the other hand, the 95% uncertainty in reversal ages is 10,000 years or less, then the ratios for slow spreading and for fast spreading differ significantly. To rapidly provide a useful modification to NUVEL-1, herein we seek an optimal single value for α by which all spreading rates used in NUVEL-1 can be multiplied.

To do so, we sought the correction that minimizes the worst error in recalibration as measured in mm/yr. By a systematic search of values between 0.9529 and 0.9573, we found that the best factor calculated to a precision of four figures is 0.9562. At the fastest "fast" rate of 160 mm/yr, this introduces a recalibration error of 0.18 mm/yr. At the fastest "medium" rate of 55 mm/yr, this introduces a recalibration error of –0.18 mm/yr. The recalibration error at slow rates is less than 0.18 mm/yr if we use an age of 2.60 Ma as estimated by *Shackleton et al.* [1990] and adopted by *Hilgen* [1991b] for the young end of chron 2A.

[1]Department of Geology and Geophysics, University of Wisconsin, Madison, Wisconsin
[2]Department of Geological Sciences, Northwestern University, Evanston, Illinois
[3]Jet Propulsion Laboratory, California Institute of Technology, Pasadena, California

Paper number 94GL02118
0094-8534/94/94GL-02118$03.00

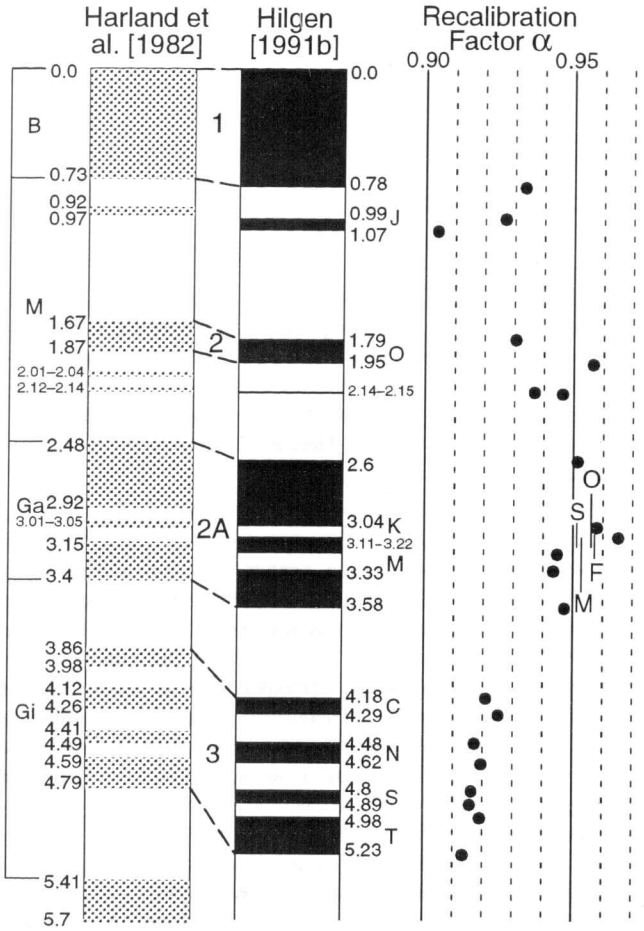

Fig. 1. Comparison of time scale used herein (i.e., that of Hilgen [1991b], which incorporates that of Shackleton et al. [1990] for 0–2.60 Ma) with the time scale of Harland et al. [1982] used in deriving NUVEL-1. The filled circles in the recalibration diagram on the right show the ratio of the age of a reversal adopted by Harland et al. [1982] to that adopted by Hilgen [1991b]. The recalibration adopted herein is entirely a consequence of these revisions to the geomagnetic reversal time scale. Note that the recalibration factors for the Gauss normal polarity chron, corresponding to anomaly 2A, which is the reference anomaly in NUVEL-1, are nearer one and therefore require less revision than those for the Brunhes, Matuyama, and Gilbert polarity chrons. The vertical line labeled "S" shows the best recalibration for profiles across slow spreading centers, the vertical line labeled "M" shows the best recalibration for profiles across medium spreading centers, and the vertical line labeled "F" shows the best recalibration for profiles across fast spreading centers. The difference (0.0058) between recalibration "S" and recalibration "F" is eight times smaller than the difference between the old and new time scales. The vertical line labeled "O" shows the optimal recalibration, which minimizes the worst error in calibration across all spreading rates and is adopted in this paper. Abbreviations for Geomagnetic Polarity Chrons: B, Brunhes Normal; M, Matuyama Reversed; Ga, Gauss Normal; Gi, Gilbert Reversed. Abbreviations for Geomagnetic Polarity Sub-Chrons: J, Jaramillo Normal; O, Olduvai Normal; K, Kaena Reversed; M, Mammoth Normal; C, Cochiti Normal; N, Nunivak Normal; S, Sidufjall Normal; T, Thvera Normal.

With this particular recalibration, we have determined a new set of angular velocities by multiplying the old angular velocities by 0.9562 (Tables 1–2). We refer to this re-calibrated set of angular velocities (i.e., those multiplied by $\alpha = 0.9562$) as NUVEL-1A. Uncertainties were similarly re-calibrated. The uncertainties in rates of rotation are simply multiplied by α (Table 2). The uncertainties in the lengths of the major and

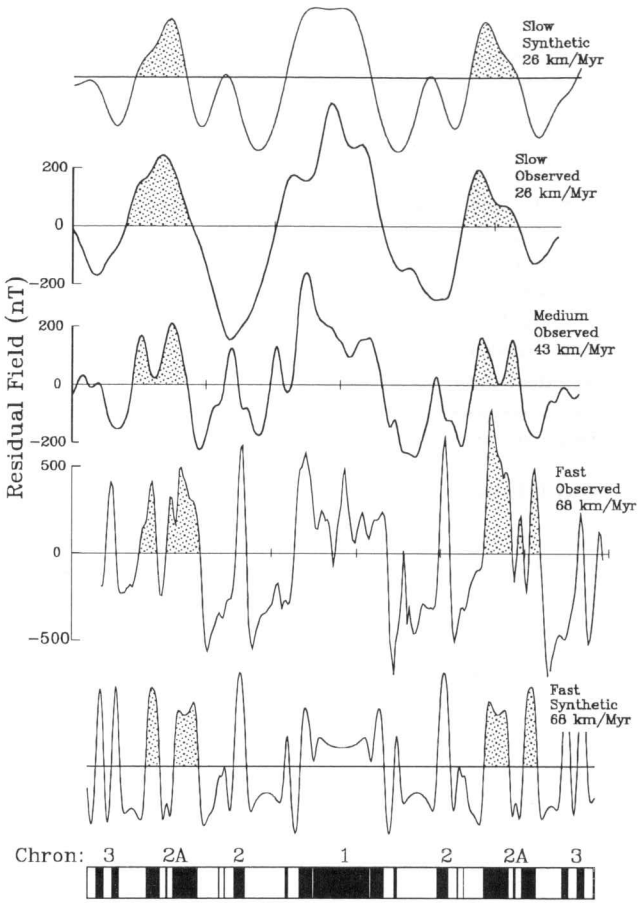

Fig. 2. Observed marine magnetic anomaly profiles across fast, medium, and slow spreading centers are compared with synthetic profiles at the indicated full spreading rates. As can be seen in both the observed and synthetic profiles, brief subchrons are better resolved within anomaly 2A at faster spreading rates. The transitions from slow to medium and from medium to fast spreading based on the character of anomaly 2A occur at slower values of spreading rate than do the analogous classifications based on spreading center morphology. The profile across a slow spreading center (Africa-North America) shows only a single positive anomaly for chron 2A with a slight inflection that may be caused by crust magnetized during the Kaena and Mammoth reversed polarity subchrons (cf. Fig. 1). The profile across an medium-rate spreading center (Central Indian Ridge) shows two positive anomalies flanking a negative anomaly in the anomaly 2A sequence. The negative anomaly resolves the combined Kaena and Mammoth polarity subchrons, but not the brief normal polarity interval between them. The profile across a fast spreading center (Southeast Indian Ridge) shows two distinct negative anomalies, corresponding to distinct Kaena and Mammoth reversed subchrons, separated by a narrow positive anomaly corresponding to the brief normal polarity interval between them.

Table 1. NUVEL-1A Angular Velocities (Pacific Plate Fixed)

Pl.	Latitude °N	Longitude °E	ω (deg-Myr^{-1})	ω_x	ω_y (radians–Myr^{-1})	ω_z
af	59.160	–73.174	0.9270	0.002401	–0.007939	0.013892
an	64.315	–83.984	0.8695	0.000689	–0.006541	0.013676
ar	59.658	–33.193	1.1107	0.008195	–0.005361	0.016730
au	60.080	1.742	1.0744	0.009349	0.000284	0.016252
ca	54.195	–80.802	0.8160	0.001332	–0.008225	0.011551
co	36.823	251.371	1.9975	–0.008915	–0.026445	0.020895
eu	61.066	–85.819	0.8591	0.000529	–0.007235	0.013123
in	60.494	–30.403	1.1034	0.008180	–0.004800	0.016760
na	48.709	–78.167	0.7486	0.001768	–0.008439	0.009817
nz	55.578	–90.096	1.3599	–0.000022	–0.013417	0.019579
sa	54.999	–85.752	0.6365	0.000472	–0.006355	0.009100
Additional Angular Velocities (Pacific Plate Fixed)						
jf[1]	35.0	26.0	0.51	0.00651	0.00317	0.00508
jf[2]	28.3	29.3	0.520	0.00671	0.00377	0.00415
ph[3]	0.	–47.	0.96	0.0114	–0.0122	0.0000
ph[4]	–1.2	–45.8	0.96	0.0116	–0.0120	0.0003
ri[5]	31.0	257.6	2.45	–0.00788	–0.03580	0.02202
sc[6]	49.1	–81.4	0.66	0.0011	–0.0075	0.0087
nnr	63.0	–72.6	0.6411	–0.00151	0.00484	–0.00997

Each named plate moves counterclockwise relative to the Pacific plate. Plate abbreviations (Pl.): af, Africa; an, Antarctica; ar, Arabia; au, Australia; ca, Caribbean; co, Cocos; eu, Eurasia; in, India; jf, Juan de Fuca; na, North America; nz, Nazca; ph, Philippine; ri, Rivera; sa, South America; sc, Scotia. The angular velocity of the no-net-rotation reference frame (nnr) relative to the Pacific plate (model NNR-NUVEL1) was recalibrated from *Argus and Gordon* [1991]. Footnotes: 1) Recalibrated from *Wilson* [1988]; this angular velocity was incorporated into model NNR-NUVEL1 [*Argus and Gordon*, 1991]. 2) Recalibrated from the more recent estimate of *Wilson* [1993b]. 3) Recalibrated from *Seno et al.* [1987]; this angular velocity was incorporated into model NNR-NUVEL1. 4) Recalibrated from the more recent estimate of *Seno et al.* [1993]. 5) Recalibrated from *DeMets and Stein* [1990]. 6) Derived from Scotia plate velocity model described by *Pelayo and Wiens* [1989]. It depends in part on spreading rates averaged over ~1.9 Ma (Anomaly 2), shorter than the 3.2-Myr averaging interval used in NUVEL-1A.

minor axes of confidence ellipses would be unchanged if the only revision were that due to the time scale revision. However, here we correct a mistake in error-ellipse length that occurred in the tables of *DeMets et al.* [1990]. In every case the corrected uncertainties are the same size as, or slightly smaller than, those given by *DeMets et al.* [1990].

Elements of the covariance matrix can be revised by multiplication by α^2. In addition to the angular velocities determined by *DeMets et al.* [1990], we give in Table 1 the recalibrated angular velocities of the Juan de Fuca plate [*Wilson*, 1988, 1993b] and of the Philippine plate [*Seno et al.*, 1987, 1993]. We have also added recalibrated angular velocities of the Rivera plate [*DeMets and Stein*, 1990] and of the Scotia plate [*Pelayo and Wiens*, 1989].

The recalibration has the unfortunate consequence of producing a new set of angular velocities that in nearly every case differ significantly from from those of NUVEL-1. This is because NUVEL-1, like all previous global plate motion models, neglects the uncertainty in rates induced by uncertainties in the geomagnetic reversal time scale. These uncertainties have been neglected not so much because they are small—although we must admit that the recent recalibrations have been surprisingly large— but because the true size of the uncertainties are still not well known. The results of *Wilson* [1993a] indicate misfits of 10,000 to 20,000 years for 1 or perhaps 2 out of 11 reversals that he examined (D. Wilson, personal communication, 1994). This suggests a tentative and approximate estimate

Table 2. NUVEL-1A Angular Velocities: Pairs of Plates Sharing a Boundary

Plate Pair	Latitude °N	Longitude °E	ω (deg-Myr^{-1})	Error Ellipse σ_{max}	σ_{min}	ζ_{max}	σ_ω (deg-Myr^{-1})
Pacific Ocean							
na-pa	48.7	–78.2	0.75	1.3	1.2	–61	0.01
ri-pa	31.0	–102.4	2.45	3.6	0.6	21	0.57
co-pa	36.8	–108.6	2.00	1.0	0.6	–33	0.05
ri-na	22.8	–109.4	1.80	1.8	0.6	–57	0.58
ri-co	6.8	–83.7	0.54	35.8	1.8	–56	0.52
co-na	27.9	–120.7	1.36	1.8	0.7	–67	0.05
co-nz	4.8	–124.3	0.91	2.9	1.5	–88	0.05
nz-pa	55.6	–90.1	1.36	1.8	0.9	–1	0.02
nz-an	40.5	–95.9	0.52	4.5	1.9	–9	0.02
nz-sa	56.0	–94.0	0.72	3.6	1.5	–10	0.02
an-pa	64.3	–84.0	0.87	1.2	1.0	81	0.01
pa-au	–60.1	–178.3	1.07	1.0	0.9	–58	0.01
eu-pa	61.1	–85.8	0.86	1.3	1.1	90	0.02
co-ca	24.1	–119.4	1.31	2.5	1.2	–60	0.05
nz-ca	56.2	–104.6	0.55	6.5	2.2	–31	0.03
Atlantic Ocean							
eu-na	62.4	135.8	0.21	4.1	1.3	–11	0.01
af-na	78.8	38.3	0.24	3.7	1.0	77	0.01
af-eu	21.0	–20.6	0.12	6.0	0.7	–4	0.02
na-sa	16.3	–58.1	0.15	5.9	3.7	–9	0.01
af-sa	62.5	–39.4	0.31	2.6	0.8	–11	0.01
an-sa	86.4	–40.7	0.26	3.0	1.2	–24	0.01
na-ca	–74.3	–26.1	0.10	24.7	2.6	–52	0.03
ca-sa	50.0	–65.3	0.18	14.9	4.3	–2	0.03
Indian Ocean							
au-an	13.2	38.2	0.65	1.3	1.0	–63	0.01
af-an	5.6	–39.2	0.13	4.4	1.3	–42	0.01
au-af	12.4	49.8	0.63	1.2	0.9	–39	0.01
au-in	–5.6	77.1	0.30	7.4	3.1	–43	0.07
in-af	23.6	28.5	0.41	8.8	1.5	–74	0.06
ar-af	24.1	24.0	0.40	4.9	1.3	–65	0.05
in-eu	24.4	17.7	0.51	8.8	1.8	–79	0.05
ar-eu	24.6	13.7	0.50	5.2	1.7	–72	0.05
au-eu	15.1	40.5	0.69	2.1	1.1	–45	0.01
in-ar	3.0	91.5	0.03	25.2	2.4	–58	0.04

The first plate moves counterclockwise relative to the second plate. Plate abbreviations are as in Table 1 plus pa, Pacific. One-sigma, two-dimensional, error ellipses are calculated in the plane tangent to Earth's surface; each is specified here by the geocentric angles subtended by its principal axes and by the azimuth (ζ_{max}, given in degrees clockwise from north) of its major axis. The rotation rate uncertainty is determined from a one-dimensional marginal distribution, whereas the lengths of the principal axes are determined from a two-dimensional marginal distribution.

of 95% uncertainty of about 20,000 years, corresponding to an additional uncertainty entirely due to time-scale uncertainties of about 0.7% of any rate. For applications for which time scale errors matter, especially for comparisons with geodetic rates, it is probably appropriate to add additional uncertainty of about this size.

Implications for the Steadiness of Plate Motion

Robbins et al. [1993] have compared rates of plate motion measured from satellite-laser ranging (SLR) and very long-baseline interferometry (VLBI) with those from NUVEL-1. The correlation coefficient between SLR and VLBI data on the one hand and NUVEL-1 on the other is 0.994, but the space geodetic rates are on average slower by 6±1%. Given that angular velocities in NUVEL-1A are 4.4% slower than those in NUVEL-1, this disrepancy shrinks to less than 2%. There is some debate about this conclusion, however. D. F. Argus (unpublished analysis, 1994) and T. Herring (oral communication, 1994) both find that VLBI data are in better agreement with the predictions of NUVEL-1 than with those of NUVEL-1A. In any event, the combined results from precise estimates of seafloor spreading, the revised geomagnetic reversal time scale, and space geodesy indicate that globally averaged plate motions are very steady, within 2% to 6%, over a time scale that ranges from several years to several Myr [*Argus and Gordon*, 1990; *Ward*, 1990; *Smith et al.*, 1990; *Robbins et al.*, 1993; *Robaudo and Harrison*, 1993; *Wilson*, 1993a; *Gordon*, 1993; *Baksi*, 1994].

For individual plate pairs, however, significant differences between the angular velocity averaged over the past few Myr and that over the past few years are emerging. In particular, D. F. Argus and R. G. Gordon (manuscript in preparation, 1994) find from VLBI data an angular velocity of the Pacific relative to the North American plate averaged over the past ~10 years that differs significantly from that presented here. In the Gulf of California, the velocity from VLBI is 5±4 mm/yr (95% confidence limits) faster than that from NUVEL-1. This faster speed might reflect a geologically recent acceleration of the Pacific-North America angular velocity or might have some other explanation, including partial accommodation of Pacific-North America motion outside the spreading rise in the Gulf of California over the past 3.2 Myr.

Acknowledgements. We thank Bernard Minster and Mike Bevis for helpful advice, Alice Gripp for pointing out a mistake in our computer code for calculating uncertainties for poles of rotation, and Doug Wilson and two anonymous reviewers for helpful reviews. D. F. Argus's part of this research was performed at the Jet Propulsion Laboratory, California Institute of Technology, under contract with NASA. This work was begun while RGG was a visiting scientist at the Laboratoire de Géodynamique Sous-Marine and has been supported by NASA grant NAG5-885 and NSF grants OCE-9218541 and EAR-9205083.

References

Argus, D. F., and R. G. Gordon, Pacific-North American plate motion from very long baseline interferometry compared with motion inferred from magnetic anomalies, transform faults, and earthquake slip vectors, *J. Geophys. Res., 95,* 17,315–17,324, 1990.

Argus, D. F., and R. G. Gordon, No-net-rotation model of current plate velocities incorporating plate motion model NUVEL-1, *Geophys. Res. Lett., 18,* 2038–2042, 1991.

Baksi, A. K., Concordant sea-floor spreading rates obtained from geochronology, astrochronology, and space geodesy, *Geophys. Res. Lett., 21,* 133–136, 1994.

DeMets, C., R. G. Gordon, D. F. Argus, and S. Stein, Current plate motions, *Geophys. J. Int., 101,* 425–478, 1990.

DeMets, C., and S. Stein, Present-day kinematics of the Rivera plate and implications for tectonics of southwestern Mexico, *J. Geophys. Res., 95,* 21,931–21,948, 1990.

Gordon, R. G., Orbital dates and steady rates, *Nature, 364,* 760–761, 1993.

Harland, W. B., A. V. Cox, P. G. Llewellyn, C. A. G. Pickton, A. G. Smith, and R. Walters, *A Geologic Time Scale,* 131 pp., Cambridge Univ. Press, New York, 1982.

Hilgen, F. J., Astronomical calibration of Gauss to Matuyama sapropels in the Mediterranean and implications for the geomagnetic polarity time scale, *Earth Planet. Sci. Lett., 104,* 226–244, 1991a.

Hilgen, F. J., Extension of the astronomically calibrated (polarity) time scale to the Miocene/Pliocene boundary, *Earth Planet. Sci. Lett., 107,* 349–368, 1991b.

Mankinen, E. A., and G. B. Dalrymple, Revised geomagnetic polarity time-scale for the interval 0–5 m.y. BP, *J. Geophys. Res., 84,* 615–626, 1979.

Pelayo, A. M., and D. A. Wiens, Seismotectonics and relative plate motions in the Scotia Sea region, *J. Geophys. Res., 94,* 7293–7320, 1989.

Robaudo, S., and C. G. A. Harrison, Plate tectonics from SLR and VLBI global data, in *Contributions of Space Geodesy to Geodynamics: Crustal Dynamics, Geodynamics Series 23,* edited by D. E. Smith and D. L. Turcotte, pp. 51–71, American Geophysical Union, Washington, 1993.

Robbins, J. W., D. E. Smith, and C. Ma, Horizontal crustal deformation and large scale plate motions inferred from space geodetic techniques, in *Contributions of Space Geodesy to Geodynamics: Crustal Dynamics, Geodynamic Series 23,* edited by D. E. Smith and D. L. Turcotte, pp. 21–36, American Geophysical Union, Washington, 1993.

Seno, T., T. Moriyama, S. Stein, D. F. Woods, C. DeMets, D. Argus, and R. Gordon, Redetermination of the Philippine sea plate motion (abstract), *Eos Trans. AGU, 68,* 1474, 1987.

Seno, T., S. Stein, and A. E. Gripp, A model for the motion of the Philippine sea plate consistent with NUVEL-1 and geological data, *J. Geophys. Res., 98,* 17,941–17,948, 1993.

Shackleton, N. J., A. Berger, and W. R. Peltier, An alternative astronomical calibration of the lower Pleistocene timescale based on ODP Site 677, *Transactions of the Royal Society of Edinburgh: Earth Sciences, 81,* 251–261, 1990.

Smith, D. E., R. Kolenkiewicz, P. J. Dunn, J. W. Robbins, M. H. Torrence, S. M. Klosko, R. G. Williamson, E. C. Pavlis, N. B. Douglas, and S. K. Fricke, Tectonic motion and deformation from satellite laser ranging to LAGEOS, *J. Geophys. Res., 95,* 22,013–22,041, 1990.

Ward, S. N., Pacific-North America plate motions: New results from very long baseline interferometry, *J. Geophys. Res., 95,* 21,965–21,981, 1990.

Wilson, D. S., Confirmation of the astronomical calibration of the magnetic polarity timescale from sea-floor spreading rates, *Nature, 364,* 788–790, 1993a.

Wilson, D. S., Confidence intervals for motion and deformation of the Juan de Fuca plate, *J. Geophys. Res., 98,* 16,053–16,071, 1993b.

D. F. Argus, Jet Propulsion Laboratory, California Institute of Technology, Pasadena, CA 91109.

C. DeMets, Department of Geology and Geophysics, University of Wisconsin, Madison, WI 53706.

R. G. Gordon and S. Stein, Department of Geological Sciences, Northwestern University, Evanston, IL 60208.

(Received Feb. 10, 1994; accepted Mar. 31, 1994.)